Journal of Molecular Catalysis B: Enzymatic 109 (2014) 1–8

Contents lists available at ScienceDirect

Journal of Molecular Catalysis B: Enzymatic

journal homepage: www.elsevier.com/locate/molcatb

A thermostable variant of *Bacillus subtilis* esterase: Characterization and application for resolving *dl*-menthyl acetate

Yi Gong, Guo-Chao Xu, Gao-Wei Zheng, Chun-Xiu Li*, Jian-He Xu*

Laboratory of Biocatalysis and Synthetic Biotechnology, State Key Laboratory of Bioreactor Engineering, East China University of Science and Technology, Shanghai 200237, China

ARTICLE INFO

Article history:
Received 30 April 2014
Received in revised form 26 July 2014
Accepted 26 July 2014
Available online 4 August 2014

Keywords:
Protein stability
Random mutagenesis
Bacillus subtilis esterase
Menthyl acetate resolution

ABSTRACT

Bacillus subtilis esterase (BSE) exhibits high activity, extraordinary substrate/product tolerance and excellent enantioselectivity in the production of *l*-menthol through enantioselective hydrolysis of *dl*-menthyl acetate. However, rapid inactivation of wild-type BSE at elevated temperatures often hampers its applications. In this work, directed evolution was used to create thermostable mutants of BSE. After screening and recombination of beneficial mutations, BSE_{V4} was chose for the best mutant. The BSE_{V4} had half-lives of 462, 248 and 0.34 h at 30, 40 and 50 °C, respectively, which were 5.6, 4.1 and 2.0 folds longer than those of BSE_{WT}. Moreover, BSE_{V4} showed an increase of 4.5 °C in T_{50}^{15} and a higher temperature optimum compared with the wild-type enzyme. In the kinetic resolution of *dl*-menthyl acetate at 1.0 M substrate loading, BSE_{V4} displayed improvements in operational stability than BSE_{WT}, leading to a 1.5-fold higher total turnover number at 45 °C. The model structure of BSE_{V4} with four mutations, built with a highly homologous *p*-nitrobenzyl esterase (PDB ID: 1QE3) as the template, revealed that the newly formed hydrogen bonds and ionic bonds were beneficial for enhancing the thermostability of BSE.

1. Introduction

Biocatalysts are increasingly employed as a greener alternative in chemical processing due to their inherent high regio- and stereoselectivity [1,2]. Despite their many favorable qualities, the insufficient stability of biocatalysts in various types of reaction media often prevents or delays their application for large-scale synthesis of fine chemicals and pharmaceuticals. Though the biocatalytic processes performed at mild temperature in aqueous medium are highly desirable, it is more practical to choose those bioprocesses catalyzed *via* more robust enzymes with higher tolerance against temperature and organic solvents which are used to increase the substrate solubility [3,4]. Hence, the development of enzymes with higher stability is increasingly needed to promote the adoption of biocatalytic synthesis in industrial production of fine or bulk chemicals.*l*-Menthol is one of the most important flavoring chemicals that are extensively used in oral products, pharmaceuticals, tobacco products and shaving products. Enantioselective hydrolysis of *l*-menthyl ester from racemic mixture mediated by a specific hydrolase in aqueous medium represents an attractive approach for the production of *l*-menthol [5,6]. We previously reported an esterase from *Bacillus subtilis* ECU0554 which could produce *l*-menthol through enantioselective hydrolysis of *dl*-menthyl acetate at 500 mM [7]. The *B. subtilis* esterase (BSE) was heterogeneously expressed in *Escherichia coli* BL21 (DE3) and exhibited high activity, extraordinary substrate/product tolerance as well as excellent enantioselectivity in the production of *l*-menthol. However, the operational stability of BSE was rather poor and the half-life was only 2.8 h under reaction conditions [8]. Thus, the industrial application was severely hampered by its insufficient stability.

Engineering the stability of biocatalysts in the view of medium optimization and enzyme modification has been extensively studied. Several methods have been used to increase the stability of enzymes with varying degrees of improvement. For example, using an immobilized lipase on solid carriers and/or in anhydrous solvents could achieve a remarkable improvement in the catalyst's activity or stability [9–11]. These methods, however, were fairly unpredictable. Moreover, the prediction of mutations with improved stability remains a challenging task in protein engineering, since the stability of proteins is a function of the overall structure and not limited to several specific sites [12]. Consequently, random mutagenesis followed by a high throughput screening in directed evolution has been

* Corresponding authors. Tel.: +86 21 6425 3002; fax: +86 21 6425 2250.
E-mail addresses: gongyi1988@126.com (Y. Gong), guochaoxu@163.com (G.-C. Xu), gaoweizheng@ecust.edu.cn (G.-W. Zheng), chunxiuli@ecust.edu.cn (C.-X. Li), jianhexu@ecust.edu.cn (J.-H. Xu).

http://dx.doi.org/10.1016/j.molcatb.2014.07.014
1381-1177/

the method of choice to engineer this particular property [13–15].

Directed evolution does not require detailed information of structures or accurate prediction on amino acid substitutions at proper sites [16]. It involves generating a vastly mutated genes library of interest by random mutagenesis such as error-prone polymerase chain reaction (epPCR) or DNA shuffling, followed by screening mutants with specified criteria for desired properties. This approach has been particularly successful in improving the thermostability of various proteins. For instance, Cherry [17] reported that the thermostability of a fungal peroxidase was dramatically enhanced by 110-fold through combining mutations from epPCR and *in vivo* shuffling with several mutants constructed by site-directed mutagenesis. A thermostable fungal cellobiohydrolase (Cel6A) [18] was engineered by random mutagenesis and recombination of beneficial mutations, which could reduce the reaction time for 10-fold in 75 °C than that of the wild type enzyme in 60 °C for avicel hydrolysis. Crystal structures showed the enhanced hydrophobic interactions and confined loop conformations contribute to the thermostability. These successful studies prompted us to generate thermostable BSE variants *via* directed evolution.

In the present work, we performed one round of directed evolution *via* random mutagenesis, in which three variants with better thermostability were identified. Then, the four substitutions in all the three variants were combined together by site-directed mutagenesis, affording BSE_{V4}. It is reported that the protein stability is related to the rigidity, while the activity is related to the flexibility [19]. We hypothesize that, increasing the rigidity might lead to a higher stability. When the rigidity increases, the flexibility could decline, which might lead to the loss of activity. Thus, our goal is to find a variant with higher thermostability, while avoiding significant loss of the activity. In our study, BSE_{V4} showed 4.7 °C increase in T_{50}^{15} than that of the wild type BSE, due to the additional introduction of ionic bonds, hydrogen bonds and hydrophobic interactions, making BSE_{V4} a more desirable biocatalyst in practical application.

2. Experimental

2.1. Materials and chemicals

Tryptone and yeast extract were obtained from Oxoid (Shanghai, China). All restriction endonucleases and T4 DNA ligase were purchased from TaKaRa (Dalian, China). The recombinant plasmids of wild type BSE (GenBank accession number: KM203868) in pET28a were the products of our previous study [8]. *E. coli* strain BL21 (DE3) from Tiangen (Shanghai, China) was used as the host strain for gene cloning and expression. The strain was routinely grown in Luria–Bertani medium at 37 °C unless stated otherwise. Kanamycin (50 μg/mL) was used for the selection of recombinant strains of *E. coli*. The pET28a expression vector was purchased from Novagen (Shanghai, China). r*Taq* DNA polymerase and the restriction enzymes (*Dpn*I, *Sal*I and *Not*I) were obtained from TaKaRa. High fidelity DNA polymerase, KOD-plus-Neo, was purchased from Toyobo (Shanghai, China).

2.2. Construction of random mutagenesis library

Random mutagenesis library was constructed by epPCR. Plasmid pET28a-BSE containing the wild type esterase gene was used as the template for the first generation of random mutagenesis. Primers 5′-ACGCGTCGACATGACTCATCAAATAGTAACG-3′ and 5′-AAGGAAAAAAGAGCGGCCGCTTATTCTCCTTTTGAAGGGAA-3′ were used as forward and reverse primers, respectively. $MnCl_2$ (0.15 mM) was used to obtain the desired level of mutagenesis rate (1–3 amino acids substitutions per protein) for the 1.5 kb parent gene. The mutagenic PCR products were gel purified, digested with *Sal*I and *Not*I, and ligated into the vector pET28a which was digested with the same two restriction enzymes. *E. coli* BL21 (DE3) cells were transformed with the resultant mutant plasmids and plated onto LB agar medium supplemented with 50 μg/mL of Kanamycin.

2.3. Screening for thermostable mutants

The screening for BSE mutants with improved thermostability was performed in 96-well microplates. The colonies harboring mutant esterase genes were transferred into 96-well plates, with several colonies carrying parent gene of BSE as a control. The colonies were grown overnight at 37 °C and 220 rpm. These plates served as master plates and they were suspended with glycerol (final concentration, 8%) and stored at −80 °C. An appropriate amount of suspension was transferred into 600 μL fresh medium, cultivated at 37 °C and 220 rpm for 2 h. Then the enzyme production was induced by addition of IPTG (final concentration, 0.5 mM). After cultivation for another 10 h at 30 °C and 220 rpm, the microplates were centrifuged at 1660 × *g* for 10 min at 4 °C, and the supernatant was discarded. The cell pellets in microplates were frozen at −80 °C for 2 h and thawed at room temperature for 20 min. To each well, 200 μL lysis buffer was added, containing 5 mM Tris–HCl (pH 8.5), 0.075% lysozyme and 1 U mL^{-1} DNase I. Then the plates were incubated for 1 h at 37 °C, and the cell suspensions were diluted by 1:5 with 5 mM Tris–HCl (pH 8.5), and centrifuged again at 1660 × *g* for 20 min. The supernatant was treated at 55 °C for 15 min in a thermal cycler and then the residual activity was measured.

The reaction mixture for screening consisted of 220 μL solution in each well [20], including 20 μL double indicators containing 0.5 mg/mL bromothymol blue and phenol red, respectively (dissolved in 5 mM Tris–HCl, pH 8.0), 80 μL 100 mM calcium chloride (dissolved in 5 mM Tris–HCl, pH 8.0), 50 μL *dl*-menthyl acetate solution (200 mM dissolved in DMF), 50 μL Tris–HCl buffer (5 mM, pH 8.0) and 20 μL enzyme solution. The color change was observed at 630 nm for 15 min at 30 °C.

2.4. Site-directed mutagenesis

Site-directed mutagenesis was used to introduce amino acids for the generation of BSE_{V4}. The site-directed mutagenesis was performed by using the KOD-Plus-Neo polymerase. The reaction mixture contained 1× buffer with 1.5 mM $MgSO_4$, 0.2 μM of each dNTP, 1 μM fw- and rev-primer, 1.0 U KOD-Plus-Neo DNA polymerase and 50 ng template DNA (BSE gene in plasmid pET28a [7]). The extension reaction was initiated by pre-heating the reaction mixture to 94 °C for 2 min. After adding the DNA polymerase, the reactions were carried out 20 cycles of heating at 98 °C for 10 s, annealing at 55–65 °C for 30 s according to the melting temperature of the primer pair, followed by elongation at 68 °C for 3.5 min. The template DNA was digested with 10 U *Dpn*I for 1 h at 37 °C. Two microliters of the plasmids containing the mutated BSE gene was transformed into 50 μL competent cells of *E. coli* BL21 (DE3).

2.5. Expression and purification of parental BSE and its variants

The entire procedure was performed at 4 °C. Cell pellets were collected, suspended in 0.1 M potassium phosphate buffer (pH 7.4, plus 0.5 M sodium chloride) and lysed by 99 rounds of sonication, each working for 6 s and stop for 4 s, with an ultrasonic oscillator (JY92-II, Scientz Biotech. Co., Ltd.). After centrifugation at 10,000 × *g* for 20 min, the supernatant was used for enzyme purification. The purification was carried out as described previously [21].

2.6. Standard enzyme assay and determination of kinetic parameters

Standard enzyme assay was carried out using *p*-nitrophenyl butyrate as the substrate, which was described previously [22]. One unit of the enzyme activity was defined as the amount of enzyme releasing 1 μmol *p*-nitrophenol per minute under the given assay conditions.

2.7. The kinetic thermal stability measurement of selected variants

The kinetic thermal stability of enzymes can be expressed as T_{50}^{15}, which is the temperature required to reduce initial activity by 50% in 15 min. Purified enzymes were diluted in phosphate buffer (100 mM, pH 8.0) to 1 mg protein per mL. The diluted enzymes were incubated for 15 min at different temperatures from 40 to 60 °C. Immediately after the heat treatment, the enzymes were placed on ice for 30 min. The residual activities of enzyme on *p*-nitrophenyl butyrate were measured.

2.8. Circular dichroism spectroscopy

The melting temperature (T_m) was measured by circular dichroism (CD) spectroscopy [23,24]. T_m of BSE and its variants were measured by Chirascan CD Spectrometer (Applied Photophysics Ltd., United Kingdom) equipped with a TC 125 temperature-control system (Quantum Northwest, China). The unfolding curves were measured from 200 to 280 nm under temperatures of 30–80 °C, using the temperature scan mode with a gradient of 1 °C/min. The measurements were performed in 10 mM sodium phosphate buffer (pH 7.4) at the concentration of 0.3 mM protein.

2.9. Half-lives of BSE_{WT} and BSE_{V4}

The half-lives of purified BSE_{WT} and BSE_{V4} at 30, 40 and 50 °C were calculated *via* exponential fitting of the data points [25]. The enzymes were diluted to 0.5 mg/mL and incubated at different temperatures at pH 8.0. Samples were withdrawn at time intervals and the residual activity was measured as described above.

2.10. Temperature optima of BSE_{WT} and BSE_{V4}

The effect of temperature on BSE activity was examined by incubating the purified enzymes with *p*-nitrophenyl butyrate (1 mM) at different temperatures ranging from 15 to 50 °C for 1 min in phosphate buffer (100 mM, pH 8.0). The activity was determined as described above.

2.11. Structural analysis

Homology-based model of BSE was constructed using the SWISS-MODEL version 8.05 [26] with the crystal structure of *p*NBE (PDB No.: 1qe3; [27]), which shared a sequence similarity of 98% with our native BSE. Visualization of the modeled structure was performed using the program PyMOL (Delano Scientific, Palo Alto, CA, USA).

2.12. Enantioselective hydrolysis of dl-menthyl acetate

Fed-batch reactions were performed in a 20-mL flat-bottomed reactor with a mixed solution of sodium phosphate buffer (9 mL, 200 mM, pH 8.0) and EtOH (1 mL). The racemic menthyl acetate (1.98 g, 10 mmol) was added to the mixed solution. The reaction was initiated by addition of the enzyme powder at a constant stirring speed (200 rpm). A thermostated water bath was used to control the reaction temperature at 30 °C, and the pH of reaction mixture was maintained at 8.0 by automatic titration with 0.5 M K_2CO_3. Samples (100 μL each) were withdrawn at different time intervals and immediately extracted with ethyl acetate (100 μL). After centrifugation (6000 × *g*, 5 min), the upper organic phase was dried over anhydrous Na_2SO_4, and analyzed by GC (CP-Chirasil-Dex CB Capillary Column, injector: 280 °C, detector: 280 °C, column: 130 °C). When the conversion rate reached 42%, another portion (10 mmol each) of substrate was fed for next batch reaction without removal of products.

3. Results

3.1. Directed evolution of BSE

In the mutagenesis and screening, approximately 10,000 clones were generated by random mutagenesis on wild-type BSE (BSE_{WT}) and screened for increased thermostability. After cultivation in 96-deep-well microplates and incubation at 55 °C for 15 min, mutants displaying a 20% higher residual activity than that of the wild-type enzyme were selected for further characterization. After the rescreening of 265 colonies, 20 variants were chosen and cultured in shake flasks for preparing the purified enzymes and evaluating thermal stabilities. Then three out of the 20 variants, designated as BSE_{V1}, BSE_{V2} and BSE_{V3}, were chosen due to their elevated thermostability and comparable enzyme activities to BSE_{WT}. Sequence analysis of BSE_{V1}, BSE_{V2} and BSE_{V3} showed that each of them had one or two amino acids substitutions to BSE_{WT}. The four beneficial mutations from the three variants were combined by site directed mutagenesis and the resultant variant, designated as BSE_{V4}, was purified and characterized (Table 1). All of the four variants displayed improved stabilities, though with a little loss of specific activities toward *dl*-menthyl acetate. Among them, BSE_{V4} showed the highest thermostability, retaining 60% of activity after incubation at 55 °C for 15 min. The increases in melting temperature (T_m) of BSE_{V1}, BSE_{V2} and BSE_{V3} were 0.7, 1.4 and 0.8 °C, respectively, as compared with that of the wild-type enzyme (T_m = 52.8 °C). Besides, BSE_{V4} showed a 2.4 °C increase in T_m compared with BSE_{WT}.

All the four positive variants showed increases in T_{50} value which is defined as the temperature at which 50% of activity is

Table 1
The melting temperatures (T_m) and T_{50}^{15} values of wild-type BSE (BSE_{WT}) and variants.

Esterase	Mutation	T_{50}^{15} (°C)	T_m (°C)	Specific activity (U mg^{-1} protein)[a]
BSE_{WT}	None	47.7 ± 0.3	52.8 ± 0.1	1335 ± 23
BSE_{V1}	K14R/L465F	50.4 ± 0.2	53.5 ± 0.1	1221 ± 16
BSE_{V2}	K391E	50.0 ± 0.1	54.2 ± 0.3	1272 ± 27
BSE_{V3}	V34I	49.8 ± 0.2	53.6 ± 0.1	1287 ± 29
BSE_{V4}	K14R/V34I/K391E/L465F	52.2 ± 0.2	55.2 ± 0.2	1251 ± 19

Data corresponds to the mean values and standard deviations of three independent experiments.
[a] The specific activity was tested toward 10 mM *dl*-menthyl acetate in 100 mM phosphate buffer (pH 8.0) at 30 °C and 220 rpm.

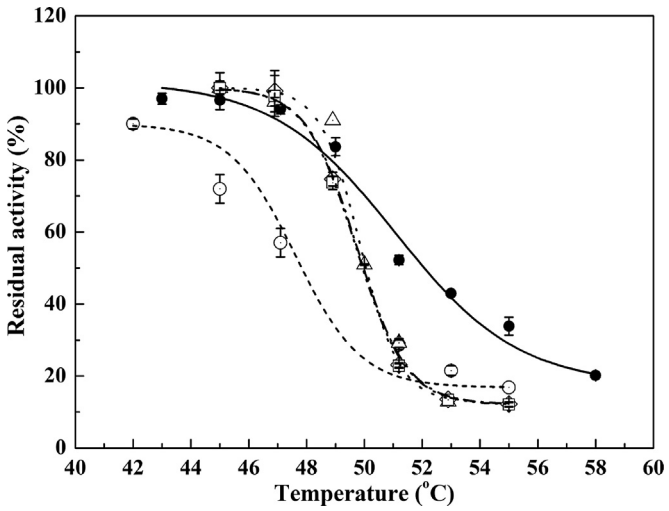

Fig. 1. Curves of thermal stability for BSE_{WT} (open circle), BSE_{V1} (open triangle), BSE_{V2} (open diamond), BSE_{V3} (open square) and BSE_{V4} (solid circle). Enzymatic activity was assayed using *p*NPB as substrate. Data points correspond to the mean values of three independent experiments.

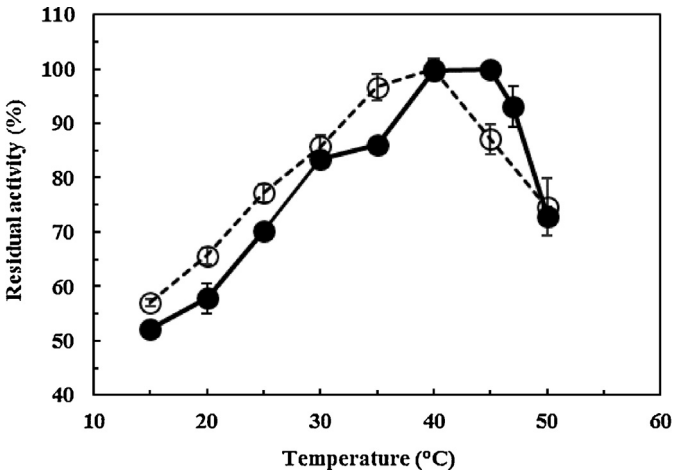

Fig. 2. Specific activities of BSE_{WT} (open circle) and BSE_{V4} (solid circle) toward *p*NPB at different temperatures. The reaction buffer was pre-incubated for 3 min at the respective temperature, followed by the hydrolysis reaction of *p*NPB for 1 min.

retained after a certain period (*e.g.*, 15 or 60 min) of incubation. In particular, the T_{50}^{15} of BSE_{V4} was 4.5 °C higher than that of BSE_{WT}. Therefore, BSE_{V4} was chosen for further research. The dynamic curves of thermal inactivation were shown in Fig. 1. Although the residual activities of BSE_{WT} and variants dropped rapidly when the temperature was raised, the slopes of curves for BSE_{V1}, BSE_{V2} and BSE_{V3} were sharper than those for BSE_{WT} and BSE_{V4}. The residual activity of BSE_{WT} started to drop from 43 °C, while those of variants decreased from an elevated temperature around 48 °C. Moreover, BSE_{V4} retained more than 50% activity at 51 °C while BSE_{WT} had only 20% activity. Furthermore, the specific activities of BSE_{WT} and BSE_{V4} for the hydrolysis of *dl*-menthyl acetate were comparable (Table 1). In this context, BSE_{V4} showed much better thermostability than those of BSE_{WT} and the other variants.

3.2. Temperature optimum

As illustrated in Fig. 2, the activity profiles of BSE_{V4} and BSE_{WT} revealed an improvement of optimum temperature from 40 to 45 °C

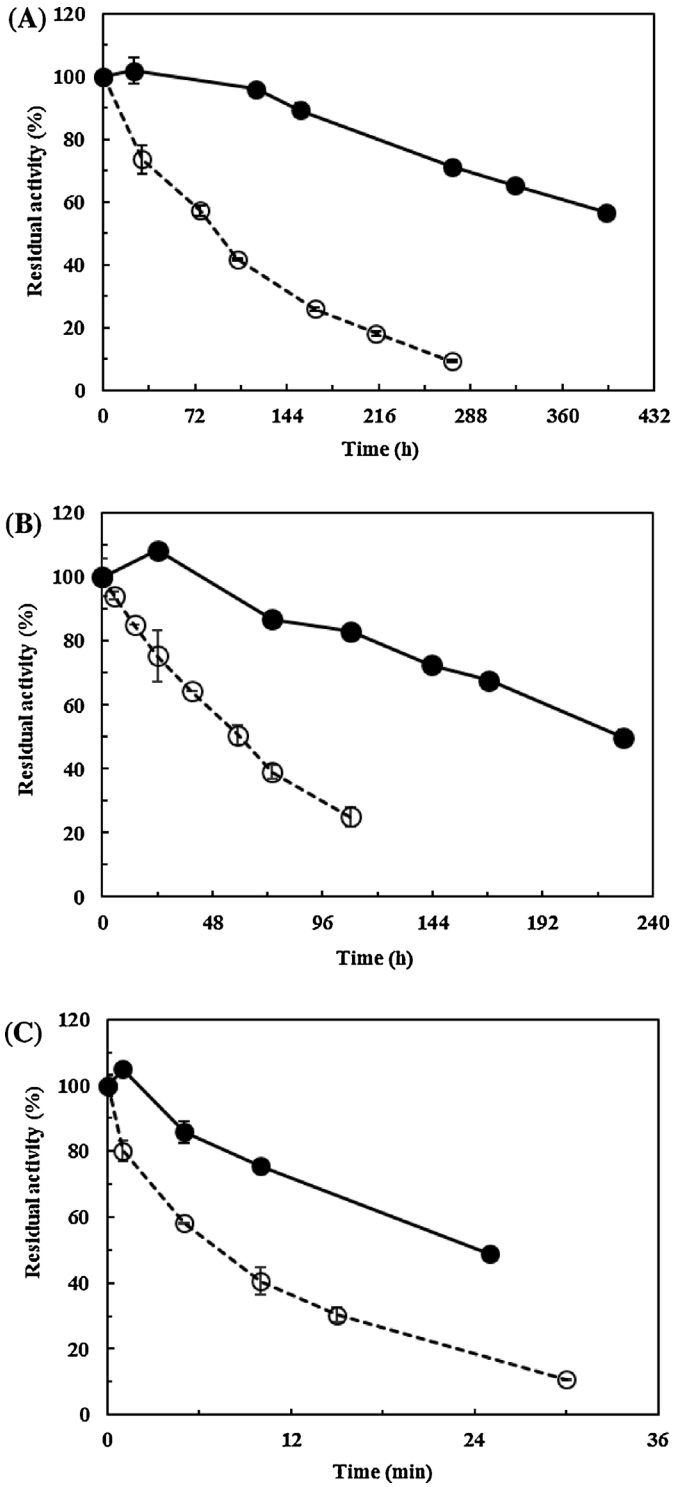

Fig. 3. Thermostability of purified BSE_{WT} (open circle) and BSE_{V4} (solid circle) at different temperatures. Purified enzyme was incubated at 30 °C (A), 40 °C (B) and 50 °C (C), respectively. Values are means of three parallel experiments.

and a wider temperature range around optimum point. The thermostability of BSE_{WT} and BSE_{V4} was further investigated in Fig. 3. The half-lives of BSE_{V4} at 30, 40 and 50 °C were 462 h, 248 h and 20.2 min, respectively, representing 5.6, 4.1 and 2.0-fold improvements compared with those of BSE_{WT}. The Arrhenius plot showed the activation energy of BSE_{V4} toward the hydrolysis of *p*NPB between 30 and 50 °C was 128 kJ/mol, in contrast to 86.9 kJ/mol for BSE_{WT}.

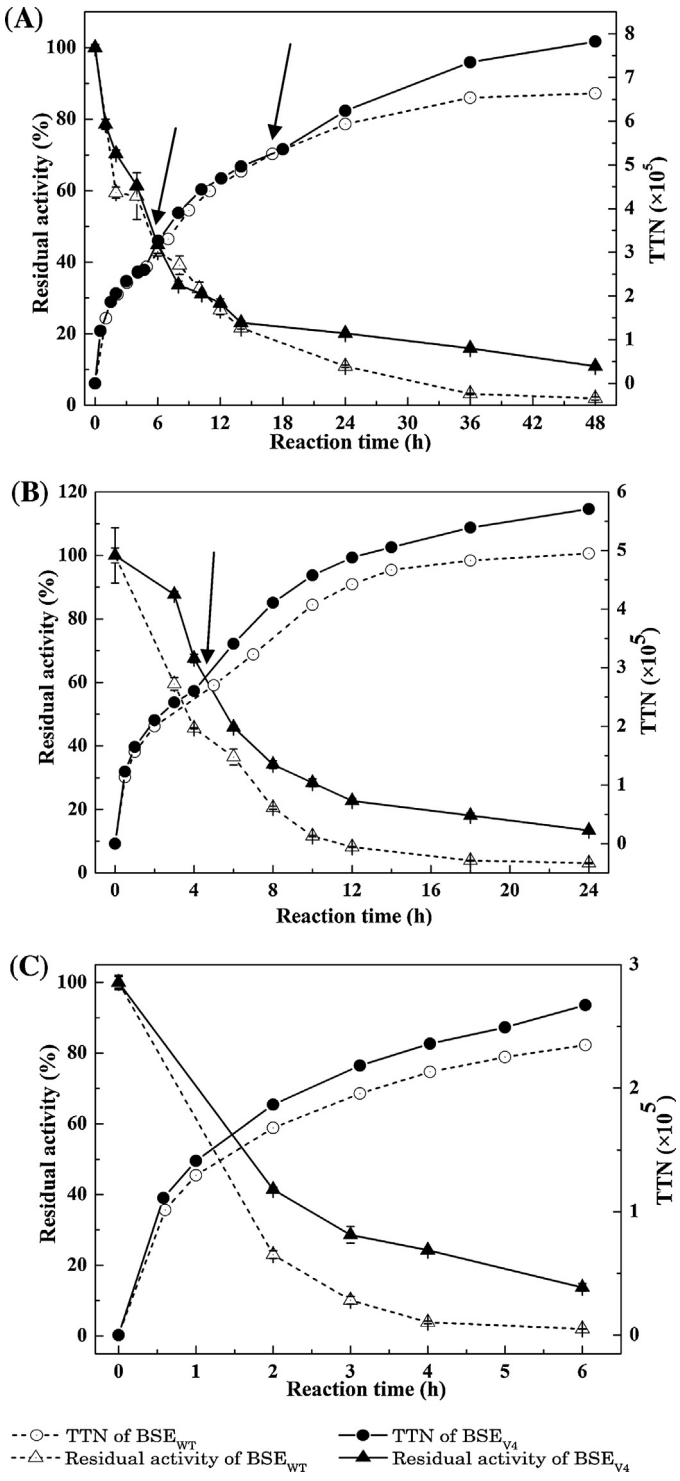

Fig. 4. Batch or fed-batch hydrolysis reactions of *dl*-menthyl acetate with BSE_{WT} or BSE_{V4} at 30 °C (A), 40 °C (B) and 45 °C (C). Total turnover numbers of BSE_{WT} (open circle, dot line) and BSE_{V4} (solid circle, solid line) were shown, in comparison to the residual activities of BSE_{WT} (open triangle, dot line) and BSE_{V4} (solid triangle, solid line) toward *p*NPB. The arrows show the time when substrate was fed.

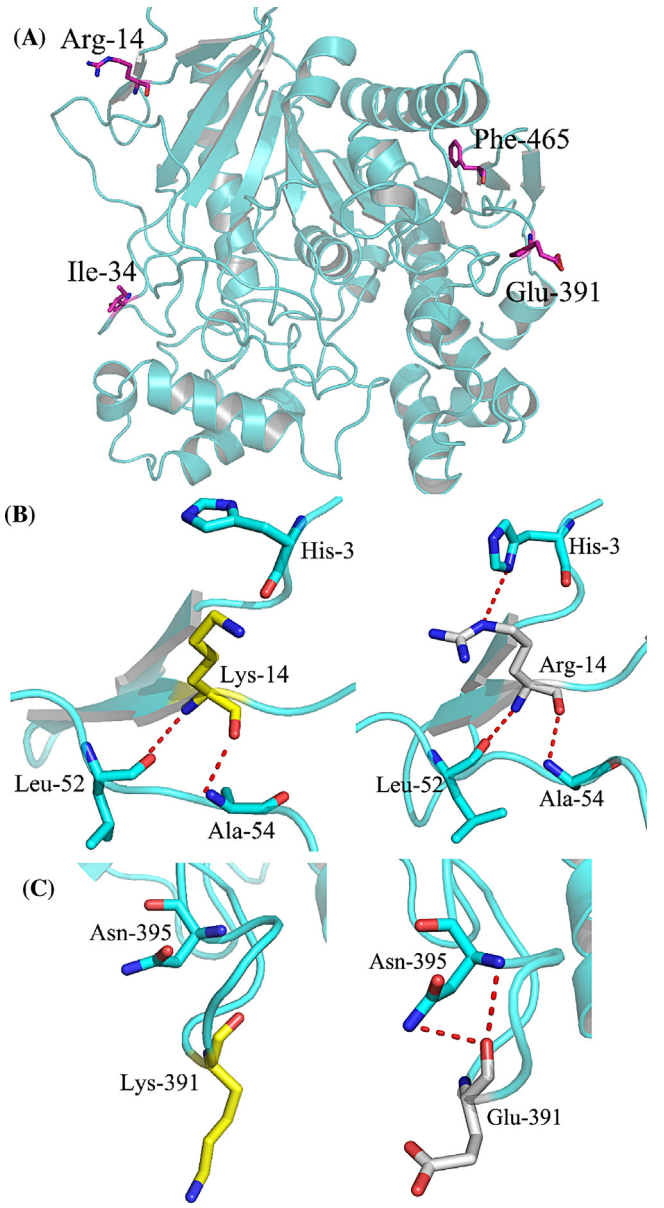

Fig. 5. The demonstration of mutation sites in BSE_{V4}. (A) Location of amino acid substitutions in the structure of BSE_{V4} constructed from *p*-nitrobenzyl esterase (PDB ID: 1QE3). (B) The substituted Arg14 was predicted to introduce hydrogen bonds to His3 and to adjacent residues, Leu52 and Ala54, respectively. (C) The substituted Lys391Glu was predicted to form two additional hydrogen bonds to Asn395. The ribbon diagrams of the three-dimensional structure were prepared using PyMOL [41]. Dotted lines indicate polar bonds.

3.3. Enantioselective hydrolysis of dl-menthyl acetate

The fed-batch reactions of BSE_{WT} and BSE_{V4} catalyzed enantioselective hydrolysis of *dl*-menthyl acetate were carried out at different temperatures as shown in Fig. 4. At 30 °C, Fig. 4A, the catalytic efficiency of BSE_{V4} was comparable to that of BSE_{WT} because both of them converted 40% of 2.0 M substrate within approximately the same time. The residual activity of the two enzymes declined to 20% after 14 h. The half-lives of the two enzymes were 462 and 83 h respectively which were far longer than 14 h, thus the declining of enzyme activity at lower temperatures should be mostly caused by the non-thermal inactivation. We believed that the shearing stress of agitation and/or the extremely high pH of the alkaline titrated to maintain the pH of reaction system contributed to the non-thermal inactivation. Although the residual activity of BSE_{V4} was only about 25% of the initial value, the third batch reaction still afforded 40% conversion after 27 h, while BSE_{WT} only gave 30% conversion under the same condition.

The higher optimum temperature and lower declining slope of BSE_{V4} indicated better stability at higher temperatures which

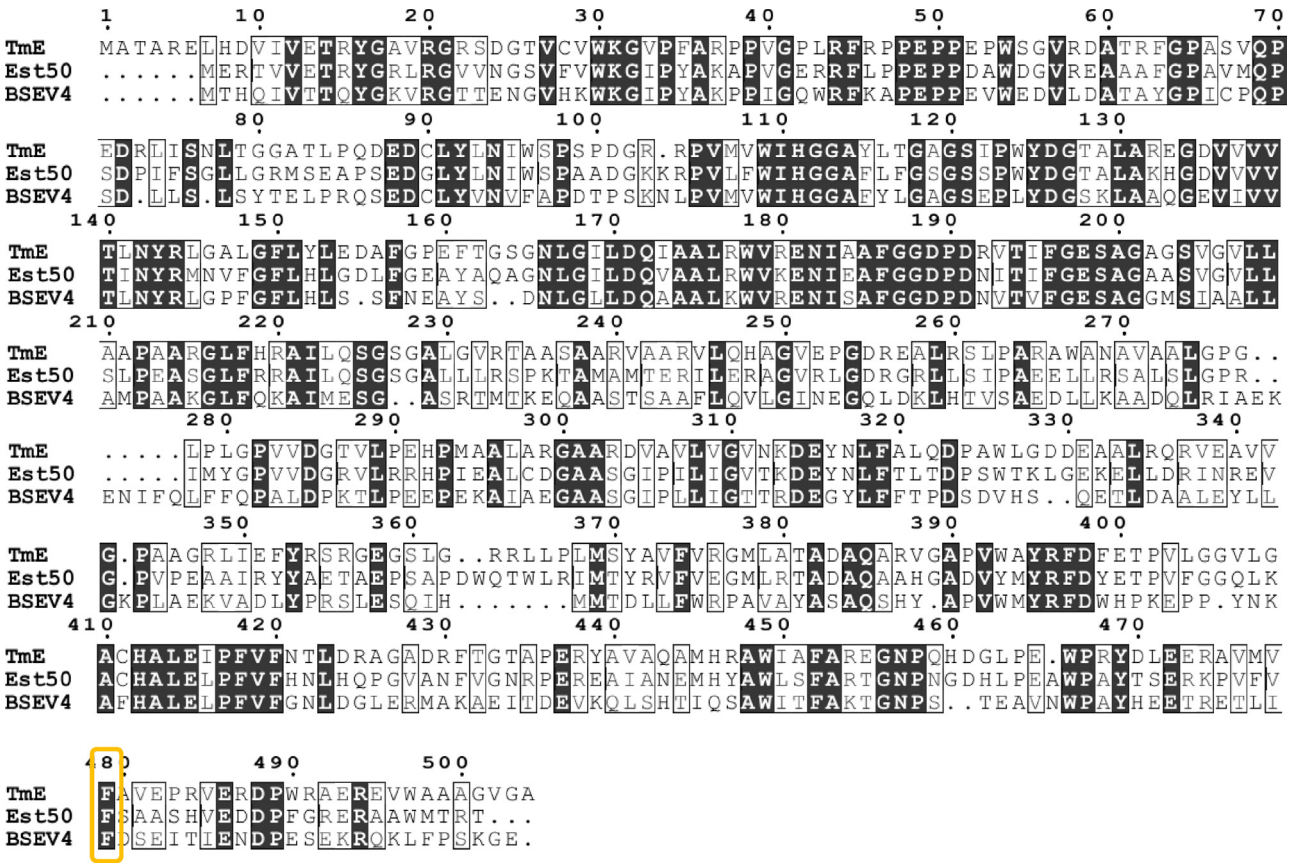

Fig. 6. The sequence alignment of BSE_{V4} with other esterases: *Tm*E from *Thermaerobacter marianensis* and Est50 from *Geobacillus kaustophilus*. The orange square indicates Phe465 in BSE_{V4}. The picture was made by ESPript.cgi Version 3.06 CGI 2.89 (session 25365) [42].

inspired us to elevate the reaction temperature to confirm its improved thermostability. Fed-batch reactions of *dl*-menthyl acetate hydrolysis by BSE_{WT} and BSE_{V4} were comparatively performed at their respective T_{opt}, 40 and 45 °C. As shown in Fig. 4B, the catalytic rate of BSE_{WT} dropped significantly during the second batch reaction due to the dropping of residual activity, while that of BSE_{V4} was kept increasing, similar to that at 30 °C. Around 8 h, the total turnover number (TTN) of BSE_{V4} reached 4.6×10^5, which was 116% of BSE_{WT}. Finally, in the end of two batches, 46% conversion was achieved for BSE_{V4} at 23 h, compared to 39% for BSE_{WT}. The TTN of BSE_{V4} was as high as 5.6×10^5, 1.1 times that of BSE_{WT}. At 45 °C, the activities of the both enzymes dropped sharply (Fig. 4C). Within 5 h, BSE_{V4} finished the first batch reaction with 42% conversion, while BSE_{WT} could not complete the conversion within 24 h. At T_{opt} of BSE_{V4}, 45 °C, the inactivation of both enzymes was rapid, while BSE_{V4} retained higher catalysis efficiency than that of the wild type. After 24 h, the TTN of BSE_{V4} was 3.58×10^5, 1.5 folds higher than that of the wild type.

4. Discussion

l-Menthol is widely used in many areas, and its output ranks the third of the spice in the world. Reflecting the strong demand for menthol in the domestic market, India, the world's largest exporter of menthol, was expected to increase the menthol production from 35,000 tons up to 42,000 tons in the period of 2012–2013. BSE can hydrolyze *dl*-menthyl acetate into *l*-menthol with high enantioselectivity, which makes it a potential catalyst for practical application. Using the method of random mutagenesis and high-throughput screening, we succeeded in improving the thermostability of the enzyme BSE. By combining the beneficial sites, we obtained the best mutant, BSE_{V4}, which displayed not only higher thermostability but also better performance in the enantioselective hydrolysis of racemic menthyl acetate under an elevated temperature (*e.g.*, 45 °C).

The stability of BSE_{WT} and variants were characterized with T_{50}^{15} and T_m values. The T_{50} measurement estimates the temperature at which 50% of the enzyme is inactivated after 15 min thermal treatment. It is often used to represent the thermal stability of enzymes, owing to allowing direct comparison of enzymes with different thermal stabilities [28,29]. The CD spectrum can be used to estimate the fractions of secondary structures [30], because it has a linear relation to the secondary structure, and the T_m is the temperature at which half of the secondary structure is unfolded. Compared to BSE_{WT}, all the variants showed enhanced resistance against relatively high temperatures. The ΔT_{50}^{15} of BSE_{V1}, BSE_{V2} and BSE_{V3} are about +2.1 °C, while that of BSE_{V4} is +4.5 °C, and ΔT_m (+2.8 °C) of BSE_{V4} is the highest among the positive variants. These results confirm that BSE_{V4} with four beneficial mutations showed improved stability against thermal treatment.

Besides, the relative half-lives of BSE_{V4} over BSE_{WT} decreased from 5.6 to 2.1-fold as the temperature of thermal inactivation rises from 30 to 50 °C. On the other hand, though the optimal temperature of BSE_{V4} is higher and the range is wider, the best activity was observed at 50 °C. Thus, BSE_{V4} is still a mesophilic enzyme. The specific activity of BSE_{V4} toward *dl*-menthyl acetate is comparable with BSE_{WT}, implying the mutations may only affect partial structure of the enzyme, and the structure of catalytic pocket remains similar.

The structure of both BSE_{WT} and BSE_{V4} were modeled for comparison. The identified amino acid substitutions in BSE_{V4} are distributed throughout the structure of a highly homologous *p*-nitrobenzyl esterase (PDB ID: 1QE3; Fig. 5A). Almost all the mutations were found on or near the surface of the enzyme, which was similar to the report of Chen and Arnold [31], except that L465F which is close to the surface of the enzyme. The site of L465F mutation, inside the enzyme, is surrounded by four aromatic residues as well as other neighboring hydrophobic residues. Therefore, the increase in thermostability may be attributed to an increase in hydrophobicity of the protein hydrophobic area. The substitution was also consistent with the result of alignment between BSE_{V4} and two thermophilic esterases (Fig. 6). Since Phe465 is under the catalytic triads (Ser189, Glu310 and His399), the increased thermostability at the cost of specific activity might be associated with a possible overall protein stability and function trade-off [32–34].

Ionic bond plays very essential role in stabilizing protein structure [35–38]. To probe the molecular basis of thermostability based on the structural predictions (Fig. 5B), we predicted that the substitution of K14R afforded one more ionic bond with histone 3 (His3), whereas Lys14 forms only two hydrogen bonds with Leu52 and Ala54. A comparison between the genomes of thermophilic and mesophilic species shows that there are more arginine and less lysine in thermophlic species than those in mesophilic species. That is because arginine can form more polar bonds with other amino acids [35]. Actually, we had done all the substitution of lysine to arginine on the surface of the protein, that was 25 substitutions in total, but no more beneficial site had been found, perhaps due to the orientation of the —NH— group.

Moreover, Lys391 forms no hydrogen bond in the wild-type enzyme, while the substitution of K391E introduces two additional hydrogen bonds between Asn395 and adjacent residues. E391 and N395 are located on a long loop region, so the newly introduced hydrogen bonds might be important in stabilizing the local structure, which helps to improve thermostability. The increase in hydrogen bonds has been suggested as one of the principal determinants in enhancing thermal stability [39,40]. The structural prediction shown in Fig. 5C indicates that the increased hydrogen bonding interactions are created by a basic residue which is located on the surface loop regions. However, the reason why the mutation of V34I can benefit the enzyme thermostability still remains unclear.

In the end, the BSE_{WT} and BSE_{V4} were applied for batch/fed-batch hydrolysis of *dl*-menthyl acetate. As a result, BSE_{V4} displayed higher TTN and better tolerance against the thermal treatment together with the shearing force of agitation and alkaline titration under all the test conditions. At 30 °C, only two batches could be finished with >40% conversion employing BSE_{WT}, while at least three batches could be achieved using BSE_{V4}. In order to further characterize the difference on the catalytic performance of BSE_{WT} and BSE_{V4}, the hydrolysis reactions were carried out at their optimum temperatures, 40 and 45 °C, respectively. At the beginning, same initial reaction rate of BSE_{WT} and BSE_{V4} was observed. Attributed to the improved thermal stability, BSE_{V4} could be operated with higher enzymatic efficiency as the supplemented of substrates. In the first batch of reaction at 40 °C, only 4 h were needed for BSE_{V4}. However, more than 5 h were required for BSE_{WT}, in spite of its higher specific activity at 40 °C. Within 24 h, two batches of substrates were hydrolyzed using BSE_{V4} with TTN of 5.6×10^5, 1.1 times of BSE_{WT}. Same catalytic performance was also discovered at even higher temperature, such as 45 °C. Additionally, the time needed for BSE_{V4} to convert 1.0 M *dl*-menthyl acetate at its T_{opt} (45 °C) was 15% shorter than that for BSE_{WT} at 40 °C (T_{opt}). All above provides evidences for the advantage of BSE_{V4} in the practical preparation of chiral menthols.

5. Conclusions

In summary, emerging directed evolution with screening and hot-spots combination, we successfully improved the thermostability of a highly active and selective esterase. Without significant loss of specific activity, the best variant BSE_{V4} displayed an increase of 4.5 °C in T_{50}^{15}. Through the homology modeling of enzyme structure, the addition of ionic bonds, hydrogen bonds and hydrophobic interactions provide further evidences to the structure stability. BSE_{V4} could survive against the inactivation at high temperature and showed better catalytic efficiency in batch/fed-batch hydrolysis of *dl*-menthyl acetate, making BSE_{V4} a more desirable and economical bioresource for practical application.

Acknowledgements

We are grateful for financial supports from the National Natural Science Foundation of China (Nos. 31200050 & 21276082), Ministry of Science and Technology, PR China (Nos. 2011AA02A210 & 2011CB710800), and the Fundamental Research Funds for the Central Universities, Ministry of Education, PR China. The authors are also indebted to Mr. Zhao who kindly eliminated many of the errors in this paper. The authors declare no commercial or financial conflict of interest.

References

[1] B.M. Nestl, B.A. Nebel, B. Hauer, Curr. Opin. Chem. Biol. 15 (2011) 187–193.
[2] S. Wenda, S. Illner, A. Mell, U. Kragl, Green Chem. 13 (2011) 3007–3047.
[3] M. Lehmann, M. Wyss, Curr. Opin. Biotechnol. 12 (2001) 371–375.
[4] C.K. Savile, J.M. Janey, E.C. Mundorff, J.C. Moore, S. Tam, W.R. Jarvis, J.C. Colbeck, A. Krebber, F.J. Fleitz, J. Brands, P.N. Devine, G.W. Huisman, G.J. Hughes, Science 329 (2010) 305–309.
[5] S. Vorlová, U.T. Bornscheuer, I. Gatfield, J.M. Hilmer, H.J. Bertram, R.D. Schmid, Adv. Synth. Catal. 344 (2002) 1152–1155.
[6] E. Brenna, C. Fuganti, F.G. Gatti, S. Serra, Chem. Rev. 111 (2011) 4036–4072.
[7] G.W. Zheng, H.L. Yu, J.D. Zhang, J.H. Xu, Adv. Synth. Catal. 351 (2009) 405–414.
[8] G.W. Zheng, J. Pan, H.L. Yu, M.T. Ngo-Thi, C.X. Li, J.H. Xu, J. Biotechnol. 150 (2011) 108–114.
[9] U.T. Bornscheuer, Angew. Chem. Int. Ed. 42 (2003) 3336–3337.
[10] M.T. Reetz, P. Tielmann, W. Wiesenhöfer, W. Könen, A. Zonta, Adv. Synth. Catal. 345 (2003) 717–728.
[11] G.W. Zheng, H.L. Yu, C.X. Li, J. Pan, J.H. Xu, J. Mol. Catal. B: Enzymatic 70 (2011) 138–143.
[12] B.J. Ryan, C.Ó. Fágáin, BMC Biotechnol. 7 (2007) 86.
[13] J.H. Kim, G.S. Choi, S.B. Kim, W.H. Kim, J.Y. Lee, Y.W. Ryu, G.J. Kim, J. Mol. Catal. B: Enzymatic 27 (2004) 169–175.
[14] W.C. Suen, N.Y. Zhang, L. Xiao, V. Madison, A. Zaks, Protein Eng. Des. Sel. 17 (2004) 133–140.
[15] V.G.H. Eijsink, S. Gåseidnes, T.V. Borchert, B. van den Burg, Biomol. Eng. 22 (2005) 21–30.
[16] M.S. Kim, X.G. Lei, Appl. Microbiol. Biotechnol. 79 (2008) 69–75.
[17] J.R. Cherry, M.H. Lamsa, P. Schneider, J. Vind, A. Svendsen, A. Jones, A.H. Pedersen, Nat. Biotechnol. 17 (1999) 379–384.
[18] I. Wu, F.H. Arnold, Biotechnol. Bioeng. 110 (2013) 1874–1883.
[19] D.G. Eynat, T.P. Agnes, E. Mikael, S.T. Dan, J. Mol. Biol. 425 (2013) 2609–2621.
[20] D. Wang, J. Wang, B. Wang, H.W. Yu, J. Mol. Catal. B: Enzymatic 82 (2012) 18–23.
[21] L.J. Wang, C.X. Li, Y. Ni, J. Zhang, X. Liu, J.H. Xu, Bioresour. Technol. 102 (2011) 7023–7028.
[22] L.L. Zhao, J.H. Xu, J. Zhao, J. Pan, Z.L. Wang, Process Biochem. 43 (2008) 626–633.
[23] J. Tian, P. Wang, S. Gao, X.Y. Chu, N.F. Wu, Y.L. Fan, FEBS J. 277 (2010) 4901–4908.
[24] C. You, Q. Huang, H.P. Xue, Y. Xu, H. Lu, Biotechnol. Bioeng. 105 (2010) 861–870.
[25] M.A. Longo, D. Combes, J. Chem. Technol. Biotechnol. 74 (1999) 25–32.
[26] F. Kiefer, K. Arnold, M. Künzli, L. Bordoli, T. Schwede, Nucleic Acids Res. 37 (2009) D387–D392.
[27] B. Spiller, A. Gershenson, F.H. Arnold, R.C. Stevens, Proc. Natl. Acad. Sci. U. S. A. 96 (1999) 12305–12310.
[28] V.G. Eijsink, A. Bjørk, S. Gåseidnes, R. Sirevåg, B. Synstad, B. van den Burg, G. Vriend, J. Biotechnol. 113 (2004) 105–120.
[29] M.T. Reetz, D.J. Carballeira, A. Vogel, Angew. Chem. Int. Ed. 45 (2006) 7745–7751.
[30] N.J. Greenfield, Nat. Protoc. 1 (2006) 2876–2890.
[31] K. Chen, F.H. Arnold, Proc. Natl. Acad. Sci. U. S. A. 90 (1993) 5618–5622.
[32] B.K. Shoichet, W.A. Baase, R. Kuroki, B.W. Matthews, Proc. Natl. Acad. Sci. U. S. A. 92 (1995) 452–456.
[33] T.B. Mamonova, A.V. Glyakina, O.V. Galzitskaya, M.G. Kurnikova, Biochim. Biophys. Acta 1834 (2013) 854–866.

[34] S. Gosavi, PLOS ONE 8 (2013) e61222.
[35] R. Das, M. Gerstein, Funct. Integr. Genom. 1 (2000) 76–88.
[36] S. Chakravarty, R. Varadarajan, Biochemistry 41 (2002) 8152–8161.
[37] S.S. Strickler, A.V. Gribenko, A.V. Gribenko, T.R. Keiffer, J. Tomlinson, T. Reihle, V.V. Loladze, G.I. Makhatadze, Biochemistry 45 (2006) 2761–2766.
[38] A.V. Gribenko, M.M. Patel, J. Liu, S.A. McCallum, C.Y. Wang, G.I. Makhatadze, Proc. Natl. Acad. Sci. U. S. A. 106 (2009) 2601–2606.
[39] S. Kumar, C.J. Tsai, R. Nussinov, Protein Eng. 13 (2000) 179–191.
[40] G. Vogt, S. Woell, P. Argos, J. Mol. Biol. 269 (1997) 631–643.
[41] LLC Schrödinger, The PyMOL Molecular Graphics System, Version 1.4.1, 2010.
[42] P. Gouet, E. Courcelle, D.I. Stuart, F. Metoz, Bioinformatics 15 (1999) 305–308.